


Article

Thiazolidinedione Derivatives: In Silico, In Vitro, In Vivo, Antioxidant and Anti-Diabetic Evaluation

Manal Y. Sameeh¹, Manal M. Khowdiary^{1,2}, Hisham S. Nassar^{3,4}, Mahmoud M. Abdelall⁴, Hamada H. Amer^{5,6}, Abdelaaty Hamed⁴  and Ahmed A. Elhenawy^{3,4,*}

- ¹ Chemistry Department, Faculty of Applied Science, Umm El Qura Branch, Makkah 24211, Saudi Arabia; Myassemih@uqu.edu.sa (M.Y.S.); mmkhowdiary@uqu.edu.sa (M.M.K.)
- ² Applied Surfactant Laboratory, Egyptian Petroleum Research Institute, Nasr City, Cairo 11727, Egypt
- ³ Department of Chemistry, Faculty of Science and Arts in Al-Mukhwah, Al-Baha University, Al Bahah 65311, Saudi Arabia; h_nassar5@yahoo.com
- ⁴ Chemistry Department, Faculty of Science, Al-Azhar University, Nasr City, Cairo 11884, Egypt; abdelall_sci@yahoo.com (M.M.A.); abdelatyhamed.1@azhar.edu.eg (A.H.)
- ⁵ Department of Animal Medicine and Infectious Diseases, Faculty of Veterinary Medicine, University of Sadat City, Sadat City 32958, Egypt; dr.hamada1435@gmail.com or h.amer@tu.edu.sa
- ⁶ Department of Chemistry, Turabah University College, Taif University, P.O. Box 11099, Taif 21944, Saudi Arabia
- * Correspondence: ahmed.elheawy@azhar.edu.eg or elhenawy_sci@hotmail.com; Tel.: +966-59-9044526

Abstract: This work aimed to synthesize a new antihyperglycemic thiazolidinedione based on the spectral data. The DFT\B3LYP\6-311G** level of theory was used to investigate the frontier molecular orbitals (FMOs), chemical reactivity and map the molecular electrostatic potentials (MEPs) to explain how the synthesized compounds interacted with the receptor. The molecular docking simulations into the active sites of PPAR- γ and α -amylase were performed. The in vitro potency of these compounds via α -amylase and radical scavenging were evaluated. The data revealed that compounds (4–6) have higher potency than the reference drugs. The anti-diabetic and anti-hyperlipidemic activities for thiazolidine-2,4-dione have been investigated in vivo using the alloxan-induced diabetic rat model along with the 30 days of treatment protocol. The investigated compounds didn't show obvious reduction of blood glucose during pre-treatments compared to diabetic control, while after 30 days of treatments, the blood glucose level was lower than that of the diabetic control. Compounds (4–7) were able to regulate hyperlipidemia levels (cholesterol, triglyceride, high-density lipoproteins and low- and very-low-density lipoproteins) to nearly normal value at the 30th day.

Keywords: thiazolidinediones; anti-diabetic; antioxidant; molecular docking



Citation: Sameeh, M.Y.; Khowdiary, M.M.; Nassar, H.S.; Abdelall, M.M.; Amer, H.H.; Hamed, A.; Elhenawy, A.A. Thiazolidinedione Derivatives: In Silico, In Vitro, In Vivo, Antioxidant and Anti-Diabetic Evaluation. *Molecules* **2022**, *27*, 830. <https://doi.org/10.3390/molecules27030830>

Academic Editor: Magda Abdellattif

Received: 19 December 2021

Accepted: 23 January 2022

Published: 27 January 2022

Publisher's Note: MDPI stays neutral with regard to jurisdictional claims in published maps and institutional affiliations.



Copyright: © 2022 by the authors. Licensee MDPI, Basel, Switzerland. This article is an open access article distributed under the terms and conditions of the Creative Commons Attribution (CC BY) license (<https://creativecommons.org/licenses/by/4.0/>).

1. Introduction

Diabetes mellitus (DM) is a common chronic health problem and around 416 million people worldwide are suffering from it. This figure is expected to reach 618 million cases by 2040 [1–4]. DM was classified into two major classes: “DMI” and “DMII” [5,6]. More than 90% of cases are diagnosed with DMII (non-insulin dependent diabetes mellitus; NIDDM). DMII is recognized by tissue resistance to the action of insulin combined with a reduction in insulin secretion because of resistance or deficiency against a beta cell, that requires insulin to control the disease [6]. Increasing glucose levels are related to raising several health problems such as cardiovascular disease, extra damage via insulin, etc. The enzyme α -glucosidase is vital in the therapeutic process and is found in secretions from salivary glands and the pancreas [7]. It belongs to the endoamylases family and is responsible for the breakdown of the α -D-(1,4) glycosidic bond in starch to obtain monosaccharides [8]. Inhibition of this enzyme is an effective protocol to reduce blood glucose level [9]. DMII patients have a two to fourfold higher risk of cardiovascular disease than non-DM patients [9]. Thiazolidinediones (TZDs) are an efficient DMII drug type [10] (Figure 1). Several TZDs' derivatives have been marketed for the treatment of

DII such as pioglitazone, rosiglitazone, ragaglitazar, balaglitazone [11] (Figure 1). Clinical studies showed that mixed therapy between α -glucosidase inhibitors and PPAR- γ -agonists (peroxisome proliferator-activated receptor [11–13]) was a helpful strategy for treatment of DMII, as acarbose combined with pioglitazone, the first prevents NIDDM and reduces the cardiovascular problem [14]) and the second acting on cardiovascular action and anti-atherosclerosis [15].

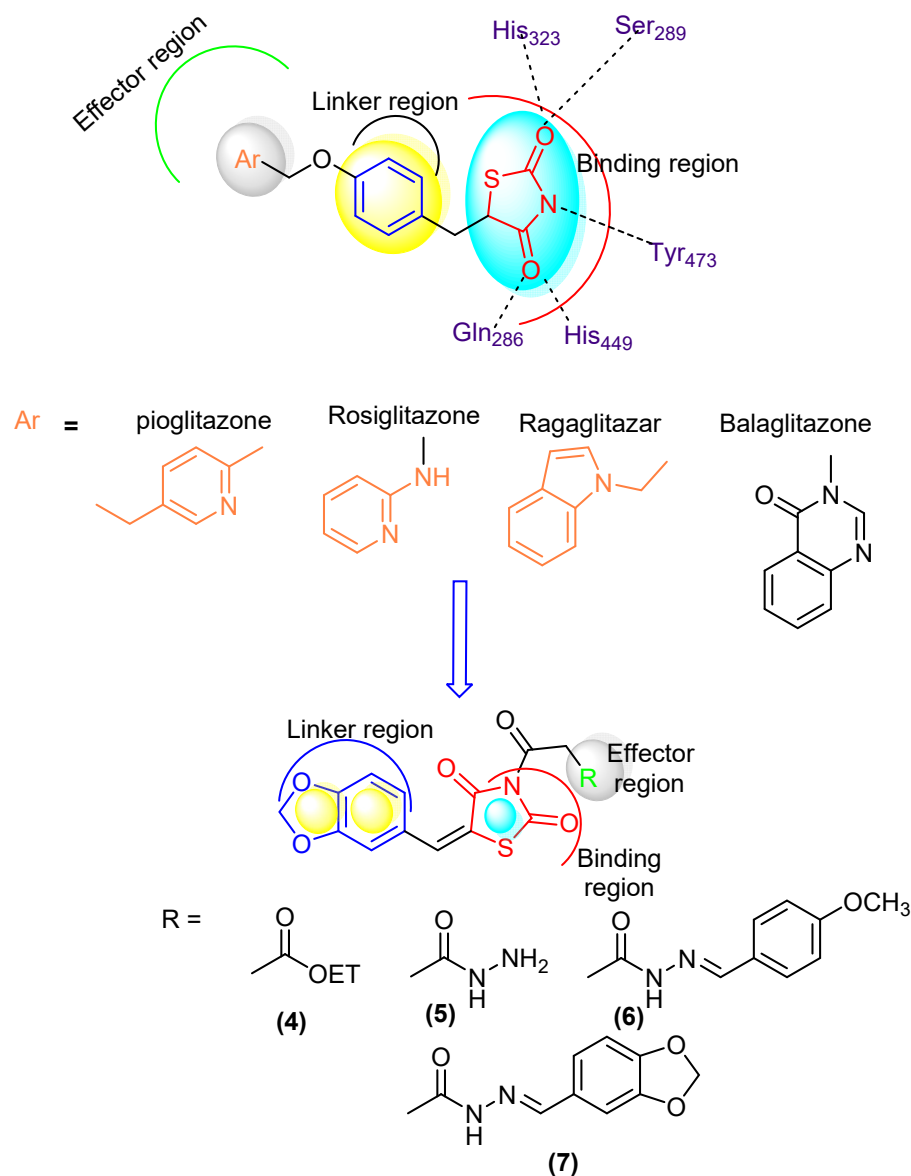


Figure 1. Designed molecule compliance of Rosiglitazone pharmacophore.

The combination thereby is also effective for older patients with hypertension and DMII [16], as well as induced-electrolyte-disturbance in DMII rats [17]. Despite the efficiency of the present drugs such as acarbose and TZDs, they can cause adverse effects such as diarrhea, hepatotoxicity, carcinogenesis, oedema, cardiac side effects and obesity [18,19]. The search for more effective novel drugs with reduced side effects is highly demanded [20]. Recently, unimolecular with multi-target drugs have been developed to handle metabolic-syndrome, as an inhibitor of Na-dependent-glucose-transporters “SGLTI” [21,22].

The 2,4-Thiazolidinediones have several potential uses as anti-cancer [23], antioxidant [24], anti-malarial [25], anti-obesity and anti-microbial agents [25,26]. In view of the above mentioned, we have reported new thiazolidinediones and evaluated their proper-

ties in silico using molecular docking and in vitro testing as α -glucosidase inhibitors and antioxidant agents, as well as studying the anti-diabetes efficacy in vivo.

2. Materials and Methods

The melting points, thin layer chromatography, IR, NMR, elemental analyses (C, H, N), and mass spectra were recorded (Supplementary Materials).

2.1. Chemistry

2.1.1. Ethyl-2-(5-(benzo[d][1,3]dioxol-5-ylmethylene)-2,4-dioxothiazolidin-3-yl)acetate (4)

Potassium salt **3** (0.1 mol) was refluxed with ethyl bromoacetate (0.1 mol) in DMF to give ester **4**. The crude product was separated and crystallized from EtOH to give ester **4** as pale-yellow crystals, yield 74%, m.p. 170–172 °C. IR (KBr): (ν/cm^{-1}) = 1692, 1736 (C=O). $^1\text{H-NMR}$ (500 MHz, DMSO- d_6) spectra δ_{H} (ppm) = 7.79 (s, 1H, CH=benzylidene), 7.20–7.14 (m, 1H, Ar-H), 7.10 (dd, J = 1.9, 0.5 Hz, 1H, Ar-H), 7.02 (d, J = 8.9 Hz, 1H, Ar-H), 6.01 (s, 2H, 2H, CH₂ of dioxole ring), 4.73 (s, 2H, NCH₂), 4.18 (q, J = 6.6 Hz, 2H, CH₃CH₂), 1.24 (t, J = 6.6 Hz, 3H CH₃). $^{13}\text{C NMR}$ (DMSO- d_6) spectra δ_{C} (ppm) = 170.18, 168.29, 167.98, 149.34, 148.33, 130.72, 128.12, 125.32, 119.76, 110.52, 109.65, 101.85, 61.46, 42.42, 14.17. Anal. Calc'd for C₁₅H₁₃NO₆S (335): C, 53.73; H, 3.88; N, 4.17. Found: C, 53.71; H, 3.84; N, 4.13.

2.1.2. 2-(5-(Benzo[d][1,3]dioxol-5-ylmethylene)-2,4-dioxothiazolidin-3-yl)acetohydrazide (5)

A mixture of ester **4** (0.1 mol) stirred with hydrazine hydrate (0.1 mol) in EtOH (30 mL) for 3 h. at 160 °C, then cooled, filtered, and crystallized from acetic acid to give ester **5** as white crystals, yield 65 %, m.p. 240–242 °C. IR (KBr): (ν/cm^{-1}) = 3385, 3251, 3147 (NH₂, NH), 1681, 1743 (C=O). MS m/z (%): 425 (M⁺, 19.3%). $^1\text{H NMR}$ (500 MHz, DMSO- d_6) δ_{H} (ppm) = 8.73 (t, J = 4.1 Hz, 1H, NH), 7.81–7.77 (m, 1H, CH= benzylidene and Ar-H), 7.20–7.14 (m, 1H, Ar-H), 7.10 (dd, J = 1.9, 0.5 Hz, 1H, NH₂), 7.02 (d, J = 8.9 Hz, 1H, Ar-H), 6.01 (s, 2H, CH₂ of dioxole ring), 4.55 (s, 2H, NCH₂). $^{13}\text{C NMR}$ (125 MHz, DMSO) δ_{C} (ppm) = 169.90, 168.76, 168.43, 149.34, 148.33, 130.68, 128.12, 125.32, 119.76, 110.52, 109.65, 101.85, 42.66. Anal. Calc'd for C₁₃H₁₁N₃O₅S (321): C, 48.59; H, 3.42; N, 13.08. Found: C, 48.55; H, 3.38; N, 13.02.

2.1.3. General Procedure for Synthesis of Hydrazones **6** and **7**

A mixture of hydrazide **5** (0.1 mol) and aromatic aldehydes (0.1 mol) in EtOH (30 mL) was heated for 3 h. The mixture was cooled, then filtered the solid product, and crystallized by the proper solvent.

2.1.4. 5-(Benzo[d][1,3]dioxol-5-ylmethylene)-3-(2-(2,4-dioxo thiazolidin-3-yl) acetyl) thiazolidine-2,4-dione (**6**)

Hydrazide **5** (0.01 mol) and piperonal (0.01 mol) in ethanol (50 mL) were refluxed for 3 h. and crystallized from EtOH/benzene to give hydrazide **6** (61%) as yellow crystals, m.p. 202–204 °C. IR (KBr): (ν/cm^{-1}) = 3142 (NH), 1689, 1736 (C=O). $^1\text{H NMR}$ (DMSO- d_6) spectra δ_{H} (ppm) = 9.65 (s, 1H, NH), 7.81–7.77 (m, 1H, CH = benzylidene), 7.69 (t, J = 0.5 Hz, 1H, CH=N), 7.30–7.02 (m, J = 8.9 Hz, 5H, Ar-H), 6.93 (d, J = 8.3 Hz, 1H), 6.01 (d, J = 5.0 Hz, 2H, dioxole ring), 4.85 (s, 2H, dioxole ring). $^{13}\text{C NMR}$ (DMSO- d_6) spectra δ_{C} (ppm) = 169.93, 168.41, 165.85, 149.34, 149.01, 148.29 (d, J = 9.2 Hz), 145.49, 130.68, 128.12, 127.95, 125.32, 121.59, 119.76, 110.52, 109.65, 108.41, 105.98, 101.85, 101.38, 42.01. Anal. Calc'd for C₂₁H₁₅N₃O₇S (453): C, 55.62; H, 3.31; N, 9.27. Found: C, 55.58; H, 3.26; N, 9.23.

2.1.5. 2-(5-(Benzo[d][1,3]dioxol-5-ylmethylene)-2,4-dioxothiazolidin-3-yl)-N'-4-methoxybenzylidene) acetohydrazide (**7**)

Hydrazide **5** (0.01 mol) and *p*-anisaldehyde (0.01 mol) in ethanol (50 mL) and refluxed for 3 h and crystallized from benzene to give hydrazide **7** (58%) as yellow crystals,

m.p. 191–193 °C. IR (KBr): (ν/cm^{-1}) = 3198 (NH), 1682, 1736 (C=O). $^1\text{H-NMR}$ (DMSO- d_6) spectra δ_{H} (ppm) = 9.67 (s, 1H, NH), 7.88 (t, J = 0.5 Hz, 1H, N=CH), 7.81–7.77 (m, 1H, CH=C), 7.61–7.55 (m, 2H, Ar-H), 7.20–7.14 (m, 1H, Ar-H), 7.12–7.08 (m, 2H, Ar-H), 7.08 (d, J = 6.9 Hz, 1H, Ar-H), 7.02 (d, J = 8.9 Hz, 1H, Ar-H), 6.01 (s, 2H, dioxole ring), 3.80 (s, 3H, OCH₃). $^{13}\text{C NMR}$ (DMSO- d_6) spectra δ_{C} (ppm) = 169.93, 168.41, 165.85, 161.47, 149.34, 148.33, 145.22, 130.68, 128.79, 128.12, 126.76, 125.32, 119.76, 114.41, 110.52, 109.65, 101.85, 55.35, 42.01. Anal. Calc'd for C₂₁H₁₇N₃O₆S (439): C, 57.40; H, 3.87; N, 9.56. Found: C, 57.34; H, 3.83; N, 9.51.

2.2. Computational Study

The Small Molecule Preparation and Protein Selection

The ligand was constructed and minimized through Density-functional theory “DFT” using B3LYP/6-311G** (Supplementary Materials). Molecular docking was achieved into the active sites of PPAR- γ (ID: 2PRG) and α -amylase (ID: 2QV4) using MOE-2019. The docking procedures are described in the Supplementary Materials.

2.3. Biological Study

2.3.1. Animals

Albino male Wistar rats (150 ± 20 g) were obtained. (Supplementary Materials).

2.3.2. Diabetes Induction

The animals were kept fasting overnight (12 h) before induction of diabetes. Diabetes was induced in rats as reported [27–31] and (Supplementary Materials).

2.3.3. Determination of the BGLs

Blood samples were obtained from the tail vein of all rats, the blood glucose levels (BGLs) were measured and monitored in all treatment groups at days 0 (basal), 2, 4, 15 and 30 as reported [32].

2.3.4. Biochemical Analysis

The blood samples (0.5 mL) were withdrawn from each rat using the retro-orbital plexus and the other steps for biochemical analysis were adapted. (Supplementary Materials).

2.3.5. The In Vitro Inhibition of α -Amylase Assay

The α -amylase activity of the probe compounds was determined using the method at [33].

2.3.6. Radical Scavenging by DPPH Method

The assay of 2,2-Diphenyl-1-picrylhydrazyl radical (DPPH) was performed according to the method at [34].

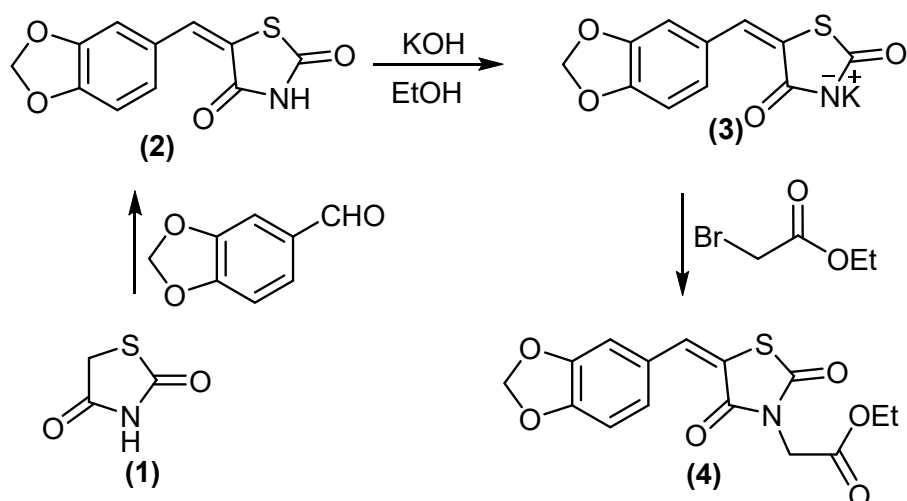
2.4. Statistical Analysis

The analysis of data is described in the Supplementary Materials.

3. Results

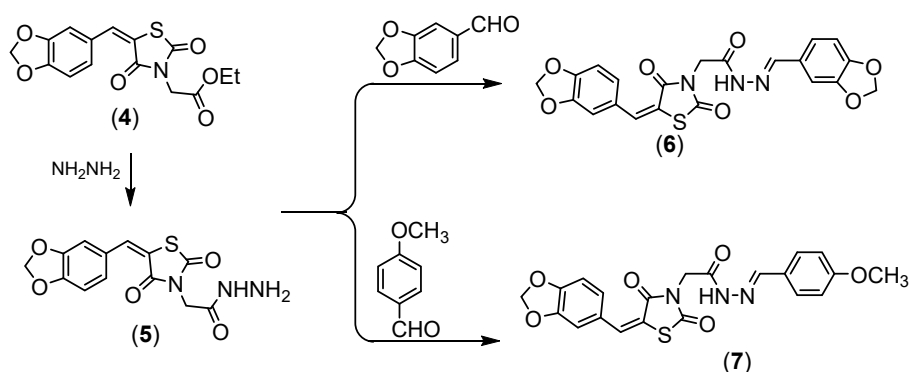
3.1. Chemistry

In a continuation of our previous work [27], we reported the synthesis of novel antidiabetic thiazolidinediones. 5-(benzo[d][1,3]dioxol-5-ylmethylene)thiazolidine-2,4-dione (**2**) treated with KOH/DMF gave potassium salt derivative (**3**). Molecule **3** was reacted with ethyl bromoacetate to afford ethyl 2-(5-(benzo[d][1,3]dioxol-5-ylmethylene)-2,4-dioxothiazolidin-3-yl)acetate (**4**), (Scheme 1). Compound **4** displayed two absorption bands attributed to 2 C=O at 1692 and 1736 cm^{-1} , while its $^1\text{H NMR}$ spectrum (DMSO- d_6) revealed the signal at δ_{H} = 4.18 ppm (2H, CH₂).



Scheme 1. Synthesis of compounds 3 and 4.

Compound 4 was hydrazinolyzed to give corresponding hydrazide derivative 5, (Scheme 2). Compound 5 succeeded in condensation with different aldehyde 5 and 6 derivatives, (Scheme 2). Compound 5 showed the absorption bands attributed to amino group at 3251 and 3147 cm^{-1} , the ethoxy resonances disappeared in NMR proton due to the appearance of the amino group at $\delta = 7.10$ ppm.



Scheme 2. Synthesis of compounds (5–7).

All the newly obtained thiazolidinediones were separated in good yields, with high purity when applied to HPLC analysis. The chemical structures were fully elucidated using IR, NMR and MS techniques.

3.2. Molecular Modeling Studies

3.2.1. Interaction Stability Based on FMO Analysis

The stability of interactions (inter- and intra-molecular) between kinase and thiazolidinedione based on FMO were examined used DFT/B3YLP/6311G** as implemented in Gaussian 09 package [35]. The FMOs included HOMO/LUMO (donating electron/accepting electron) can decide the interaction rout between compounds and kinase (Figure 2). The FMOs gap was used to examine the chemical reactivity of the molecule [36]. The growing level of HOMO energy reflects the powerful ability for providing electrons with high susceptibility to oxidation, and vice versa [37,38]. The value for E_{HOMO} was sorted by decreasing order $5 > 7 > 6 > 4$ (Table 1). The HOMO sector localized over benzodioxol in all compounds, at the same time the LUMO cloud condensed over benzodioxol ring.

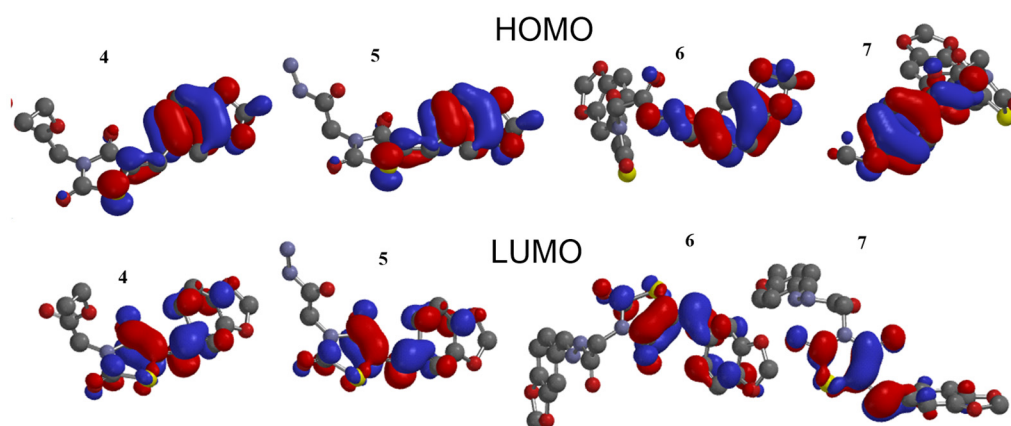


Figure 2. HOMO and LUMO orbitals density for compounds (4–7).

Table 1. Energetic global reactivity parameters for compounds (4–7) at DFT with a B3LYP\6-311G** Basics sets.

	4	5	6	7		4	5	6	7
HOMO	−8.78	−9.27	−9.14	−9.20	ω_i	−3.087	−3.15	−3.232	−3.215
LUMO	−1.19	−1.11	−1.29	−1.22	$\mu+$	−6.882	−7.123	−7.203	−7.401
ΔG	7.59	8.16	7.85	7.98	$\mu-$	6.24	6.405	6.02	6.05
IP	8.78	9.27	9.14	9.2	$\omega-$	2.8	2.70	3.20	2.902
I	1.19	1.11	1.29	1.22	$\omega+$	9.04	9.196	9.536	9.408
A	3.795	4.08	3.925	3.99	ω^\pm	1.313	1.272	1.328	1.305
η	0.263	0.245	0.254	0.25	ΔN_{\max}	2.627	2.544	2.657	2.611
S	−4.985	−5.19	−5.215	−5.21					
χ	3.274	3.3	3.464	3.401					

The HOMO and LUMO have a negative energy indicating the intramolecular electron cloud transfer as thiazolidine-2,4-dione→benzodioxole. The energy gap ΔG is vital for examination of the stability for the biomolecule in the receptor. The low value of the ΔG for the tested compounds postulates a promising interaction between FMO and kinase [37].

The chemical reactivity for 4–7 was computed in (Table 1), like; η , hardness (quantifies the resistance to change in the electron distribution in a collection of nuclei and electrons); S, softness (reciprocal of hardness) [39]; μ , chemical potential; χ , electronegativity strength [40]; the $\mu-$, electron donating power; $\mu+$, the amount of catching electron; $\omega-$, electron donating capacity; $\omega+$, the amount of electron accepting; ω^\pm , net electrophilicity (a relative power between electron accepting and electron donating) [41]; ωI , electrophilicity index in ground state; ω_i^{VS} , electrophilicity index in valance state [42]. These parameters represented in terms I, ionization potential and A, electron affinity [41]. The amount of electron was measured by reactivity index term “ ΔN_{\max} ”, which represented as a stabilization energy, when a system acquired an additional electronic charge from the environment during chemical reaction, the previous terms represented in Equations (S1)–(S11), Supplementary Materials.

The soft nucleophiles and hard electrophiles connected with the raising ΔG , that can measure the stability index (the low energy-gap molecule has improved the polarizability, softness, chemical reactivity and nucleophilicity), and vice versa. Low softness values (\sim −4.9–5.21 ev.) for the synthesized compounds (4–7) related to its high reactivity via biological environment (Table 1).

All compounds (4–7) showed almost similar ($\omega+$ and $\mu+$) values. The data proved that the ester and hydrazide fragments can improve electron donation to kinase. In addition,

these compounds (4–7) have a very promising electrophilicity value ($\omega^{\pm} = 1.27$ to 1.3 eV), that figured a good electrophilicity of 4–7, which may enhance the chances of attack over a polar-active site of the receptor.

3.2.2. The MEP Analysis

The MEP was mapped to figure the balance between repulsive interaction (nucleophilic ability) and attractive interaction (electrophilic reactivity) (Figure 3). The orange, yellow and red colors depict the negative power (great electron density area). The colors near to blue shift figured a positive potential, and green color represented intermediate potential ability. MEPs showed that the electron density covered over backbone for compounds (4–7). The expansion of a red region for these compounds related to electrophilic potency. The variety in shading of MEPs is related to diversity of electrostatic potential values that can be attributed to expanding electrostatic interactions' ability and identification between substrate and receptor [43]. Furthermore, the conformational analysis and optimization geometry for compounds (4–7) were performed at DFT and mapped (Figures S1–S4, Supplementary Materials). Thiazolidine-2,4-dione ring is stabilized with benzo[d][1,3]dioxole in planarity modes for compounds (4 and 5) and is perpendicular in case of compounds (6 and 7). From Figure 3B, one can observe the same spatial arrangement of the chemical structures (4–7).

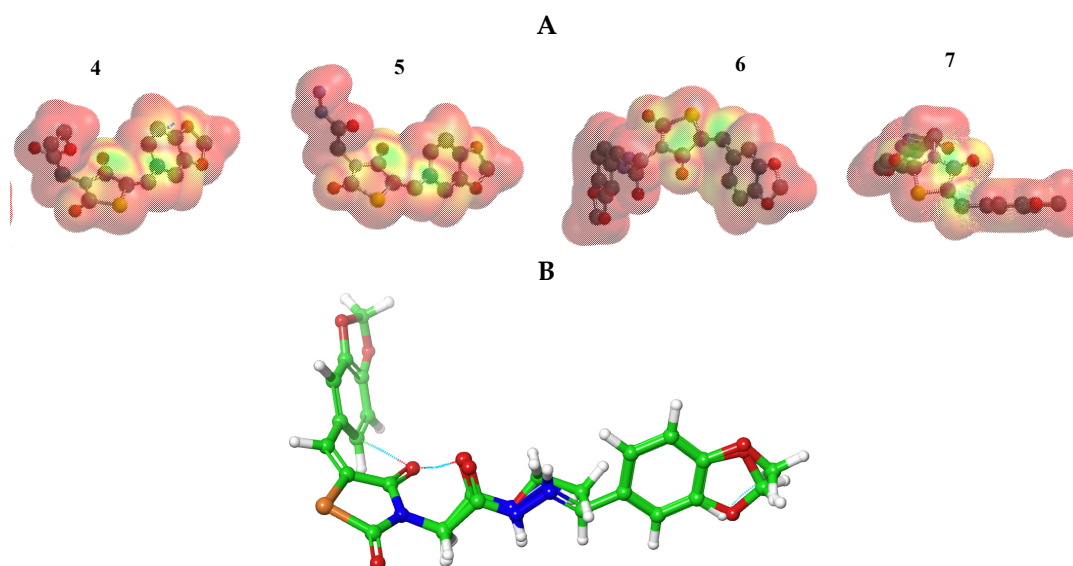


Figure 3. (A) MEP plot of synthesized compounds (4–7); (B) Overlapping the chemical structures for all compounds (4–7).

3.3. Docking Studies

The molecular docking was performed via PPAR- γ and α -amylase to examine a regulation action for compounds (4–7). The ligand–protein interaction was estimated based on the gold score function in MOE.2019 [44]. From the X-ray of kinases and its regulators [33,45], we can notice that the TZDs to be a kinase-regulator should include the following structural elements: TZD head, lipophilic side chain and aromatic linker. The probe compounds docked successfully into the reported active sites (CYS 285, GLU233, HIS 449, SER299, HIS323, CYS285, ASP300, Arg195), (Asp300, Glu233 and Asp197) for (PPAR- γ , PDB: 2PRG [46]) and (α -amylase, PDB:2QV4 [47]), respectively. Then, the (MMFF94) force field was applied for optimization of the docked pose. To evaluate the binding affinity “BE” for the tested TZs, we used the highest MOE scoring function with the lowest RMSD (Table 2). For further confirmation of the BE we examined the inhibition constant (Ki) [48], the bioactivity factor and the Ligand-Efficiency (LE) [49].

Table 2. Docking energy scores (kcal/mol) derived from the MOE for (3–6, 9 and 11).

Cpd.	4	5	6	7
2PRG				
ΔE	−8.25	−8.43	−6.59	−6.14
RMSD	2.23	2.70	1.98	2.95
$E_{\text{Int.}}$	17.12	11.59	−25.84	15.12
$E_{\text{H.B.}}$	−25.24	−14.25	−20.75	−15.75
L.E	−3.46	−2.08	−3.20	−6.50
Ki(μM)	0.12	0.11	0.13	0.13
2QV4				
E_{place}	−7.32	−7.46	−6.74	−6.14
RMSD	2.29	1.15	1.95	2.95
$E_{\text{Int.}}$	17.94	7.30	−23.29	15.12
$E_{\text{H.B.}}$	−15.45	−30.40	−24.48	−15.75
L.E	−5.674	−6.487	−3.456	−6.463
Ki(μM)	0.127	0.130	0.117	0.107

ΔE : Free binding energy of ligand-pose; E_{place} : Free binding energy of ligand-receptor; $E_{\text{Int.}}$: Binding-Affinity energy of ligand-receptor; H.B.: Energy H-bonding between protein and ligand; RMSD; The root mean square deviation of the docking pose compared to the co-crystal ligand position.

In **PPAR- γ** : Compounds (4 and 5) have the highest BE (−8.25 and −8.43 Kcal/mol.), with promising Ki (0.12 and 0.11 μM), respectively (Table 2). Compound 6 has BE higher than 7. All compounds showed a normal range of Ki and LE bioactivity parameters as [50]. All compounds (4–7) interacted with kinase in the same manner for original inhibitor.

In **α -amylase**: Compounds (4 and 5) also displayed the highest BE (−7.32 and −7.42 Kcal/mol.) with lowest inhibition constant Ki (0.12 and 0.13 μM), respectively (Table 2). All compounds showed a normal range of bioactivity parameters as Ki and LE [50]. Compounds 4 and 5 interacted with Asp300 residue by formation of H-bond, while compound 5 formed one more H-bond with important amino acid ASP197 (Figure 4).

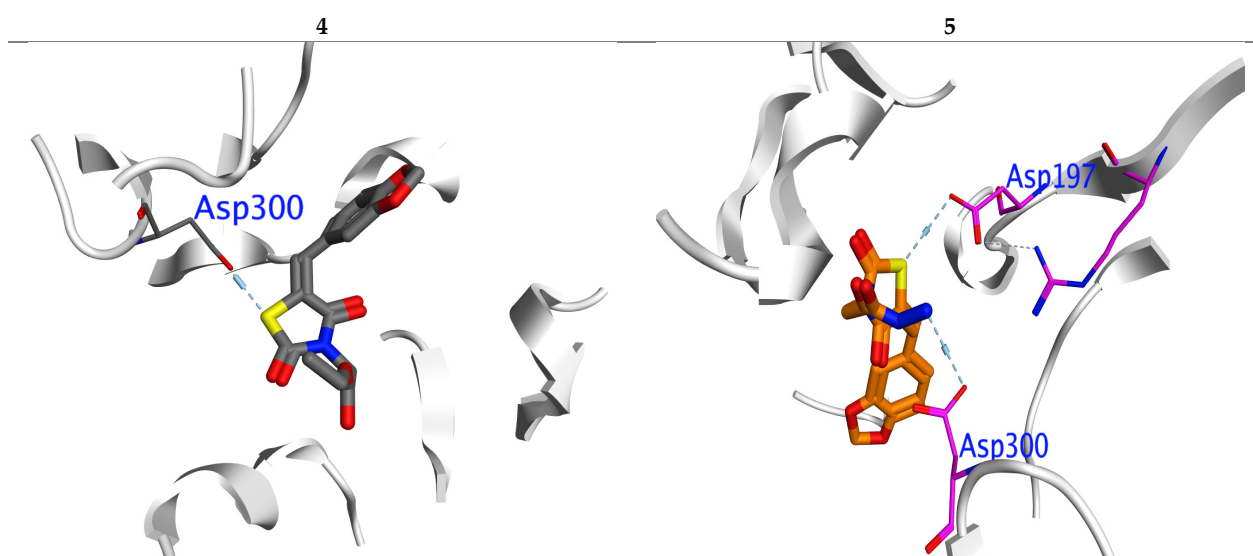


Figure 4. Interaction between ligands 4 and 5 with 2QV4 binding sites in which blue lines represent hydrogen bonding interaction.

3.4. Biological Study

3.4.1. The In Vitro α -Amylase Inhibitory Profile

The inhibitory potential was examined for compounds (4–7) against α -amylase enzyme. We used six different concentrations (5, 10, 15, 20, 30 and 40 $\mu\text{g}/\text{mL}$) for this test. The concentrations were plotted against inhibition to determine IC_{50} (concentration required to inhibit 50% of enzyme) using non-linear regression method (Figure 5). Compounds (4–6) showed higher inhibitory potential ($\text{IC}_{50} = 11.8$ to 21.34 $\mu\text{g}/\text{mL}$) than “STD” standard acarbose ($\text{IC}_{50} = 24.1$ $\mu\text{g}/\text{mL}$). Meanwhile 7 with $\text{IC}_{50} = (57.34$ $\mu\text{g}/\text{mL}$) showed lower potency than acarbose with significant ($p < 0.05$) when compared to positive control. The parent compound which bore the ester (4), hydrazide (5) and benzodioxole (6) corners had a more promising activity than acarbose (Figure 5). On the other hand, the inhibition potency decreased by the introduction of the methoxyphenyl fragment to the hydrazone in the molecular skeleton, as in 7. This efficiency can be attributed to increasing hydrophilicity, which can interact with hydrophobic part of the active site.

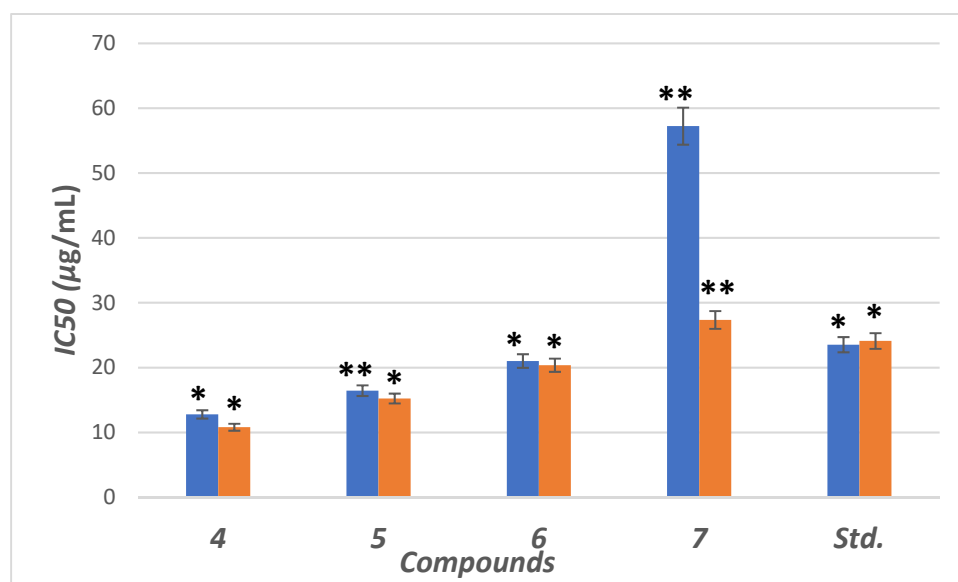


Figure 5. IC_{50} in ($\mu\text{g}/\text{mL}$) for 4–7 compared to ascorbic and acarbose, respectively, as standard drugs against DPPH radical (blue column) and α -amylase enzyme (orange column), respectively. Data analyzed by one way ANOVA followed by LSD test and expressed as mean \pm SEM from five observations; stars represent change as compared to control; ** indicates $p < 0.01$ and * shows $p < 0.05$.

3.4.2. The In Vitro Antioxidant Activity

The antioxidant compounds can protect β -cells from reactive oxygen species (ROS) and, therefore, can prevent diabetes induced by ROS [51]. In addition, ROS induces oxidative stress that leads to lipid peroxidation, protein glycation/oxidation and nitration, enzyme inactivation and DNA damage, which leads to the development of various pathological conditions such as diabetes mellitus (DM) and neurodegenerative diseases, which in turn can be neutralized by the presence of endogenous or exogenous antioxidant systems [52,53].

The antioxidant activity was examined for the hybrids (4–7) using the stable DPPH assay. The antioxidant results from different concentrations (0.16, 0.8, 4, 20, 40, 200 and 1000 $\mu\text{g}/\text{mL}$) were represented in Figure 5 as IC_{50} value (concentration of compound is essential for rising 50% of reducing power for H-donating or radical scavenging). The effect of the scavenging is rising in the trend 4 > 5 > 6 > STD > 7. Compounds (4–6) possess antioxidant activity higher than STD (ascorbic acid), while 7 has lower scavenging activity than STD. The compounds with a terminal ester 5 and hydrazide 6 groups showed the highest scavenging potency with $\text{IC}_{50} = 12.78$ and 16.44 $\mu\text{g}/\text{mL}$. After blocking the hydrazide group by aldehyde motifs in compounds 6 and 7, the activity was decreased.

High scavenging activity may be due to the stabilization of the lone pair in the conjugated system by the presence of terminal ester or hydrazide.

3.4.3. The In Vivo Regulation of Blood Glucose Level

Oral anti-hyperglycemic activity was evaluated for compounds 4–7 by an alloxan-induced diabetic rat model. Diabetes was successfully induced in the rats under investigation, as verified by their raised blood glucose level (BGL) compared with the normal control rats. The BGL was monitored for each tested compound at three different doses (50, 100 and 250 mg/Kg) and for five experimental period durations (0, 2, 4, 15, 30 days).

All of the compounds 4–7 didn't show obvious reducing of the BGL during the pretreatments compared to DC, while after 30 days, compounds 5–7 showed a decrease in the BGL at all concentrations (Figure 6). Compound 7 only reduced BGL significantly during the 4th, 15th and 30th days of the treatments at 250 mg/Kg, while compound 5 organized the BGL more than 6 at these concentrations during the 15th and 30th days. Compound 4 failed to control BGL in all durations of the experiment at 250 mg/Kg compared to the DC.

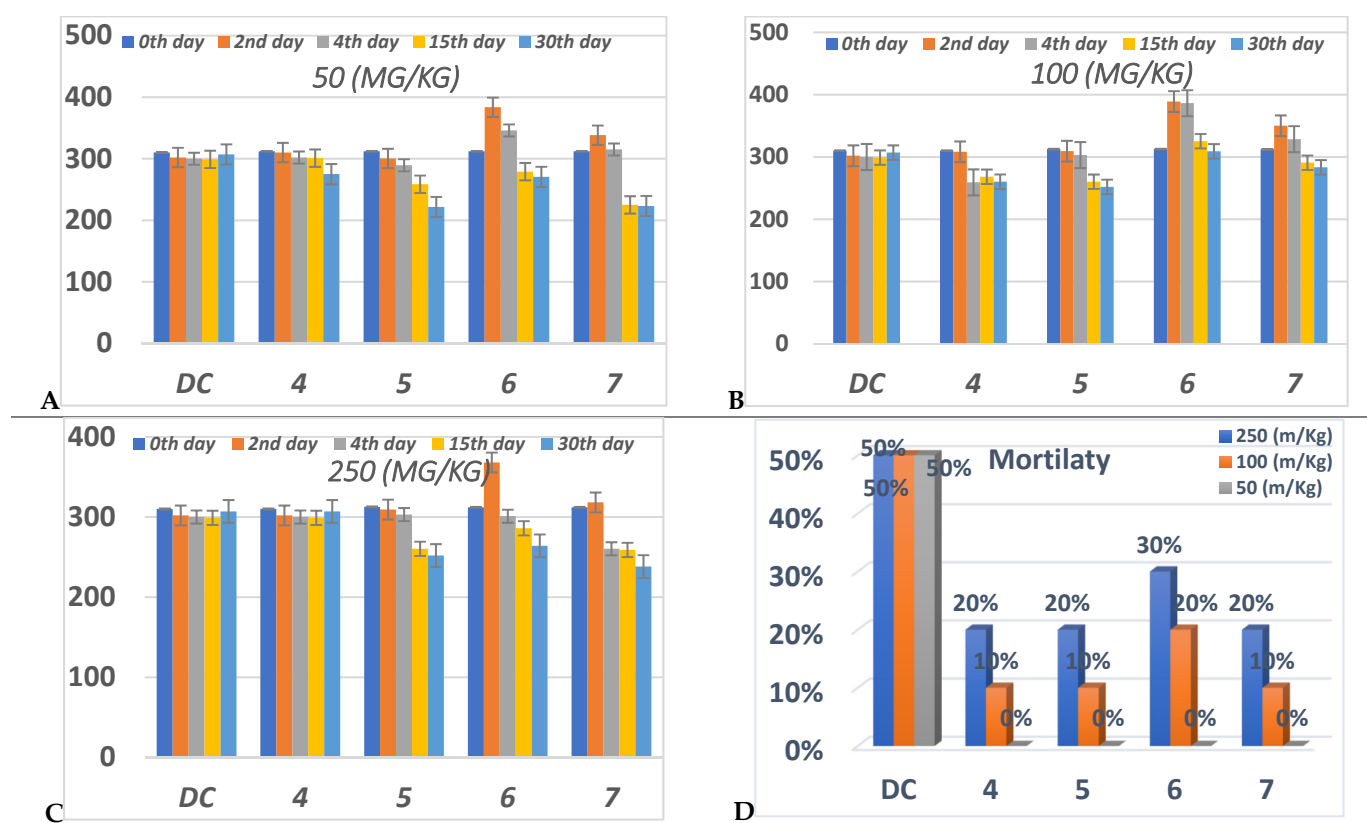


Figure 6. Anti-diabetic effect in three different concentrations, (A) 50 (mg/Kg), (B) 100 (mg/Kg) (C) 250 (mg/Kg), and (D) percent of mortality after 30 days for each group of compounds (4–7) in comparison to diabetic control “DC”. Data analyzed by one way ANOVA followed by LSD test and expressed as mean \pm SEM from different observations.

On the other hand, at 100 mg/Kg concentration, only compounds 4 and 5 achieved a significance decrease in the BGL via DC at the 15th and 30th days; during these days compound 7 displayed an insignificant decrease in the BGL. Compound 6 increased the BGL rather than DC per all of the experiments at 100 mg/Kg.

At 50 mg/Kg concentration; compounds 5–7 showed the highest reduction of the BGL at the 15th and 30th days. Compound 7 showed the highest percentage in the BGL reduction at the 15th and 30th days compared to the other members. Conversely, compared

to the DC, compounds **4** at the 2nd, 4th and 15th days and **6** at the 2nd and 4th days have suffered from controlling the BGL.

From (Figure 6), all compounds didn't exhibit any mortality at 50 mg/Kg during the whole experiment.

3.4.4. Lipid Profile

The serious side effect related to diabetes is hyperlipidemia [54,55]. The insulin deficiency promotes adipocytes to generate fatty acid, hepatic phospholipids and cholesterol [56,57]. Thus, the levels of cholesterol (CH), triglyceride (TG), high (HDL), low (LDL) and very low (VLDL) density lipoproteins, in serum for alloxan-loaded diabetes have been measured at 50 mg/Kg concentration (Figure 7). All lipid parameters for all tested compounds have ($p < 0.05$) compared to the diabetic control group (Figure 7).

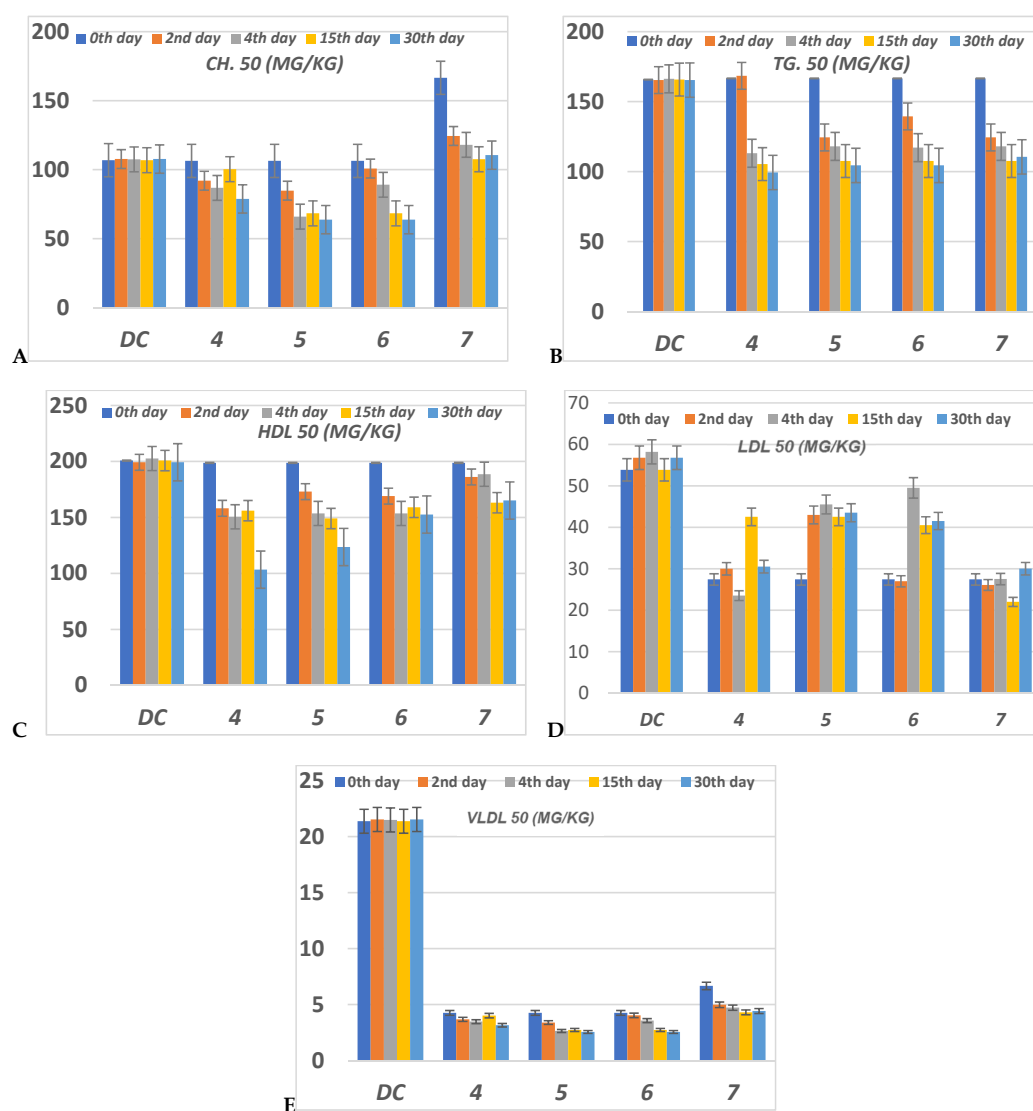


Figure 7. The level of (A) CH (Cholesterol); (B) TG (Triglyceride); (C) HDL (High density lipoprotein); (D) LDL (Low density lipoprotein) and (E) VLDL (Very low density lipoprotein) in serum of hyperglycemic loaded rats. 50 (mg/Kg) at 0th day (pre-drug values), 2nd and 4th days (post-drug values) for each group of compounds 4–7 and compared to diabetic control (DC). Data analyzed by one way ANOVA followed by LSD test and expressed as mean \pm SEM from five observations.

The serum CH level in compounds 4–6 has decreased to a lower level than DC value during the 4th, 15th and 30th days of the experiment (Figure 7). Compounds 5 and 6 at the

15th and 30th days showed the best reduction of the CH level. At the 2nd and 4th days, compound 6 showed moderate reduction, while compound 5 showed moderate reduction value at the 2nd day but this value was enhanced during the 4th day. Compound 4 showed moderate regulation of the CH value per all the experimental time. Compound 7 represented the worst CH level from all compounds at all experimental times (Figure 7).

All compounds 4–7 during the experimental period succeeded in reducing the TG level compared to DC. The TG level for compounds 4–7 was decreased lower than DC animals by the percentage between 0–37.66% along all the experimental periods 0th–30th days. Compound 4 only failed to regulate the TG level lower than the DC level at the 2nd day, while in the other periods for treatment it was the most effective member in lowering CH level to a percentage between 33.77–37.66%. Compounds 5–7 were able to decrease the TG level with 16–30% more than DC (Figure 7).

Serum HDL level was improved for all compounds 4–7 in contrast to the DC. The HDL value was significantly reduced to a nearly normal level. The best member groups were 4 and 5 in all experimental periods because of their achieving a reduced percentage, about 15% to 50% lower than DC. During the whole period of the experiment, the serum LDL was enhanced to normal level for all group members (Figure 7). Compounds 5 and 6 have monitored the level of serum VLDL to be lower than normal value at 15th and 30th days. All compounds 4–7 didn't regulate VLDL levels to be of normal level at the 0th, 4th and 15th days, but they achieved a promising reduction in LDL compared to DC. Compound 4 had regulated VLDL of infected rats to nearly normal value during the 2nd, 14th and 30th days while at the 0th and 15th days it failed to do so.

4. Conclusions

An antihyperglycemic compound, based on the thiazolidinedione scaffold, was synthesized and characterized. The FMOs and global reactivity data indicated that the intramolecular charge transfer takes place between the thiazolidine-2,4-dione and benzodioxole corner in two directions. The MEP for these compounds represented that they have promising electrophilicity, that may enhance the attacking chance over a polar active site of the receptor. The molecular docking into the PPAR- γ and α -amylase showed the high binding-affinity for the synthesized compounds and may be a suitable regulator for both kinases. The in vitro inhibition potency via the α -amylase and scavenging radical were evaluated and represented that the parent compound bearing these corners ester 4, hydrazide 5 and benzodioxole 6 are more efficient than reference drugs. This efficacy decreased in the presence of methoxyphenyl group 7 in the molecular skeleton. The anti-diabetic and anti-hyperlipidemic activities in vitro showed that all of the used concentrations for compounds 4–7 didn't show an obvious reduction in the BGL during pre- and post-treatments compared to DC, while after the 30th days of treatment, they decreased the BGL at all concentrations. The ester 5 hybrid was the most potent regarding the regulation of BGL at different concentrations at the 30th day. All compounds didn't exhibit any mortality at 50 mg/Kg concentration during the whole experiment. Moreover, all compounds enhanced hyperlipidemic levels nearly to the normal level.

Supplementary Materials: The following are available online, Figure S1: The geometrical optimization for compound 4., Figure S2: The geometrical optimization for compound 5, Figure S3: The geometrical optimization for compound 6., Figure S4: The geometrical optimization for compound 7, Table S1: The conformational analysis for selected theoretical geometrical parameters of compound 4; Table S2: The conformational analysis for selected theoretical geometrical parameters of compound 5; Table S3: The conformational analysis for selected theoretical geometrical parameters of compound 6; Table S4: The conformational analysis for selected theoretical geometrical parameters of compound 7. Equations (S1)–(S10): Quantum equations.

Author Contributions: Project administration M.Y.S., Conceptualization, M.Y.S. and A.A.E.; methodology, H.S.N. and M.M.K.; software, A.A.E.; validation, M.M.A. and A.A.E.; formal analysis, A.A.E.; investigation, M.Y.S.; resources, M.M.K.; data curation, H.S.N.; writing—original draft preparation,

A.A.E.; writing—review and editing, H.H.A., A.A.E. and A.H.; visualization, A.A.E.; supervision, A.A.E. All authors have read and agreed to the published version of the manuscript.

Funding: The authors would like to thank the Deanship of Scientific Research at Umm Al-Qura University for the continuous support. This work was supported financially by the Deanship of Scientific Research at Umm Al-Qura University to Dr. Manal Semih (Grant Code: 18-SCI-1-03-0012).

Institutional Review Board Statement: The study was conducted according to the guidelines of the declaration of Helsinki and approved by the national research center in Egypt.

Informed Consent Statement: Not applicable.

Data Availability Statement: The data presented in this study are available on request from the corresponding author.

Acknowledgments: The authors would like to thank the Deanship of Scientific Research at Umm Al-Qura University for the continuous support.

Conflicts of Interest: The authors declare no conflict of interest.

Sample Availability: Samples of the compounds are not available from the authors.

References

1. Zimmet, P.; Alberti, K.G.; Shaw, J. Global and societal implications of the diabetes epidemic. *Nature* **2001**, *414*, 782–787. [[CrossRef](#)] [[PubMed](#)]
2. Wild, S.H.; Roglic, G.; Green, A.; Sicree, R.; King, H. Global prevalence of diabetes: Estimates for the year 2000 and projections for 2030: Response to Rathman and Giani. *Diabetes Care* **2004**, *27*, 2569. [[CrossRef](#)]
3. Bhutani, R.; Pathak, D.P.; Kapoor, G.; Husain, A.; Kant, R.; Iqbal, M.A. Synthesis, Molecular modelling studies and ADME prediction of benzothiazole clubbed oxadiazole-Mannich bases, and evaluation of their Anti-diabetic activity through in-vivo model. *Bioorganic Chem.* **2018**, *77*, 6–15. [[CrossRef](#)] [[PubMed](#)]
4. Cho, N.H.; Shaw, J.E.; Karuranga, S.; Huang, Y.; da Rocha Fernandes, J.D.; Ohlrogge, A.W.; Malanda, B. IDF Diabetes Atlas: Global estimates of diabetes prevalence for 2017 and projections for 2045. *Diabetes Res. Clin. Pract.* **2018**, *138*, 271–281. [[CrossRef](#)] [[PubMed](#)]
5. Diamond, J. The double puzzle of diabetes. *Nature* **2003**, *423*, 599–602. [[CrossRef](#)]
6. King, H.; Aubert, R.E.; Herman, W.H. Global burden of diabetes, 1995–2025: Prevalence, numerical estimates, and projections. *Diabetes Care* **1998**, *21*, 1414–1431. [[CrossRef](#)]
7. American Diabetes Association. 9. Pharmacologic approaches to glycemic treatment: Standards of Medical Care in Diabetes—2019. *Diabetes Care* **2019**, *42* (Suppl. 1), S90–S102. [[CrossRef](#)]
8. Tangphatsornruang, S.; Naconsie, M.; Thammarongtham, C.; Narangajavana, J. Isolation and characterization of an α -amylase gene in cassava (*Manihot esculenta*). *Plant Physiol. Biochem.* **2005**, *43*, 821–827. [[CrossRef](#)]
9. Del Prato, S.; Chilton, R. Practical strategies for improving outcomes in T2DM: The potential role of pioglitazone and DPP4 inhibitors. *Diabetes Obes. Metab.* **2018**, *20*, 786–799. [[CrossRef](#)]
10. Brownlee, M. Biochemistry and molecular cell biology of diabetic complications. *Nature* **2001**, *414*, 813–820. [[CrossRef](#)]
11. Nanjan, M.J.; Mohammed, M.; Kumar, B.P.; Chandrasekar, M.J. Thiazolidinediones as antidiabetic agents: A critical review. *Bioorganic Chem.* **2018**, *77*, 548–567. [[CrossRef](#)] [[PubMed](#)]
12. Brownlee, M.; Hirsch, I.B. Glycemic variability: A hemoglobin A1c-independent risk factor for diabetic complications. *JAMA* **2006**, *295*, 1707–1708. [[CrossRef](#)] [[PubMed](#)]
13. Chiasson, J.L.; Josse, R.G.; Gomis, R.F.; Hanefeld, M.; Karasik, A.; Laakso, M. Acarbose for the prevention of Type 2 diabetes, hypertension and cardiovascular disease in subjects with impaired glucose tolerance: Facts and interpretations concerning the critical analysis of the STOP-NIDDM Trial data. *Diabetologia* **2004**, *47*, 969–975. [[CrossRef](#)] [[PubMed](#)]
14. Yokoyama, H.; Katakami, N.; Yamasaki, Y. Recent advances of intervention to inhibit progression of carotid intima-media thickness in patients with type 2 diabetes mellitus. *Stroke* **2006**, *37*, 2420–2427. [[CrossRef](#)]
15. Brownlee, M. The pathobiology of diabetic complications: A unifying mechanism. *Diabetes* **2005**, *54*, 1615–1625. [[CrossRef](#)]
16. Xiao, B.; Xiao, Y.; Ning, H.; Han, X.; Li, W.; Ma, Y.; Zhao, N.; Du, G.; Dong, Y.; Jung, J.H. In vitro dual-target activities and in vivo antidiabetic effect of 3-hydroxy-N-(p-hydroxy-phenethyl) phthalimide in high-fat diet and streptozotocin-induced diabetic golden hamsters. *Med. Chem. Res.* **2020**, *29*, 2077–2088. [[CrossRef](#)]
17. Khatoun, H.; Najam, R. Effects of Rosiglitazone and Acarbose (with and without Cornstarch Diet) on serum electrolytes in diabetic rats. *J. Appl. Pharm. Sci.* **2012**, *2*, 50. [[CrossRef](#)]
18. Bennett, W.L.; Maruthur, N.M.; Singh, S.; Segal, J.B.; Wilson, L.M.; Chatterjee, R.; Marinopoulos, S.S.; Pahan, M.A.; Ranasinghe, P.; Block, L. Comparative effectiveness and safety of medications for type 2 diabetes: An update including new drugs and 2-drug combinations. *Ann. Intern. Med.* **2011**, *154*, 602–613. [[CrossRef](#)]

19. Sims, H.; Smith, K.H.; Bramlage, P.; Minguet, J. Sotagliflozin: A dual sodium-glucose co-transporter-1 and-2 inhibitor for the management of Type 1 and Type 2 diabetes mellitus. *Diabet. Med.* **2018**, *35*, 1037–1048. [CrossRef]
20. Frias, J.P.; Nauck, M.A.; Van, J.; Kutner, M.E.; Cui, X.; Benson, C.; Urva, S.; Gimeno, R.E.; Milicevic, Z.; Robins, D.; et al. Efficacy and safety of LY3298176, a novel dual GIP and GLP-1 receptor agonist, in patients with type 2 diabetes: A randomised, placebo-controlled and active comparator-controlled phase 2 trial. *Lancet* **2018**, *392*, 2180–2193. [CrossRef]
21. Garcia-Vallvé, S.; Guasch, L.; Tomas-Hernández, S.; del Bas, J.M.; Ollendorff, V.; Arola, L.; Pujadas, G.; Mulero, M. Peroxisome Proliferator-Activated Receptor γ (PPAR γ) and Ligand Choreography: Newcomers Take the Stage: Miniper-spective. *J. Med. Chem.* **2015**, *58*, 5381–5394. [CrossRef] [PubMed]
22. May, L.D.; Lefkowitz, J.H.; Kram, M.T.; Rubin, D.E. Mixed hepatocellular–cholestatic liver injury after pioglitazone therapy. *Ann. Intern. Med.* **2002**, *136*, 449–452. [CrossRef] [PubMed]
23. Okumura, T. Mechanisms by which thiazolidinediones induce anti-cancer effects in cancers in digestive organs. *J. Gastroenterol.* **2010**, *45*, 1097–1102. [CrossRef] [PubMed]
24. Devji, T.; Reddy, C.; Woo, C.; Awale, S.; Kadota, S.; Carrico-Moniz, D. Pancreatic anticancer activity of a novel geranylgeranylated coumarin derivative. *Bioorganic Med. Chem. Lett.* **2011**, *21*, 5770–5773. [CrossRef]
25. Naim, M.J.; Alam, M.J.; Ahmad, S.; Nawaz, F.; Shrivastava, N.; Sahu, M.; Alam, O. Therapeutic journey of 2, 4-thiazolidinediones as a versatile scaffold: An insight into structure activity relationship. *Eur. J. Med. Chem.* **2017**, *129*, 218–250. [CrossRef]
26. Bahare, R.S.; Ganguly, S.; Agrawal, R.; Dikshit, S.N. Thiazolidine: A Potent Candidate for Central Nervous System Diseases. *Cent. Nerv. Syst. Agents Med. Chem. (Former. Curr. Med. Chem.-Cent. Nerv. Syst. Agents)* **2017**, *17*, 26–29. [CrossRef]
27. Elhenawy, A.; Salama, A.A.; All, M.M.A.; Alomri, A.A.; Nassar, H. Synthesis, characterization and discovery novel anti-diabetic and anti-hyperlipidemic thiazolidinedione derivatives. *Int. J. Pharm. Sci. Rev. Res.* **2015**, *31*, 23–30.
28. Hofmann, P. *Arvi Rauk: “Orbital Interaction Theory of Organic Chemistry”*; Wiley & Sons: New York, NY, USA, 1994; ISBN 0-471-59389-3.
29. Fukui, K. Role of frontier orbitals in chemical reactions. *Science* **1982**, *218*, 747–754. [CrossRef]
30. Wildman, S.A.; Crippen, G.M. Prediction of physicochemical parameters by atomic contributions. *J. Chem. Inf. Comput. Sci.* **1999**, *39*, 868–873. [CrossRef]
31. Parr, R.G.; Chattaraj, P.K. Principle of maximum hardness. *J. Am. Chem. Soc.* **1991**, *113*, 1854–1855. [CrossRef]
32. Parr, R.G.; Pearson, R.G. Absolute hardness: Companion parameter to absolute electronegativity. *J. Am. Chem. Soc.* **1983**, *105*, 7512–7516. [CrossRef]
33. Lamaka, S.V.; Zheludkevich, M.L.; Yasakau, K.A.; Serra, R.; Poznyak, S.; Ferreira, M. Nanoporous titania interlayer as reservoir of corrosion inhibitors for coatings with self-healing ability. *Prog. Org. Coat.* **2007**, *58*, 127–135. [CrossRef]
34. Parr, R.G.; Szentpaly, L.V.; Liu, S. Electrophilicity index. *J. Am. Chem. Soc.* **1999**, *121*, 1922–1924. [CrossRef]
35. Frisch, M.; Trucks, G.; Schlegel, H.; Scuseria, G.; Robb, M.; Cheeseman, J.; Scalmani, G.; Barone, V.; Mennucci, B.; Petersson, G. *Gaussian 09, Revision D. 01*; Gaussian, Inc.: Wallingford, CT, USA, 2013.
36. Luque, F.J.; López, J.M.; Orozco, M. Perspective on “Electrostatic interactions of a solute with a continuum. A direct utilization of ab initio molecular potentials for the prevision of solvent effects”. In *Theoretical Chemistry Accounts*; Springer: Berlin/Heidelberg, Germany, 2000; pp. 343–345.
37. Sundriyal, S.; Viswanad, B.; Ramarao, P.; Chakraborti, A.K.; Bharatam, P.V. New PPAR γ ligands based on barbituric acid: Virtual screening, synthesis and receptor binding studies. *Bioorganic Med. Chem. Lett.* **2008**, *18*, 4959–4962. [CrossRef]
38. Siddiqui, S.A.; Rasheed, T.; Faisal, M.; Pandey, A.K.; Khan, S.B. Electronic structure, nonlinear optical properties, and vibrational analysis of gemifloxacin by density functional theory. *J. Spectrosc.* **2012**, *27*, 185–206. [CrossRef]
39. Willson, T.M.; Brown, P.J.; Sternbach, D.D.; Henke, B.R. The PPARs: From orphan receptors to drug discovery. *J. Med. Chem.* **2000**, *43*, 527–550. [CrossRef]
40. Maurus, R.; Begum, A.; Williams, L.K.; Fredriksen, J.R.; Zhang, R.; Withers, S.G.; Brayer, G.D. Alternative Catalytic Anions Differentially Modulate Human α -Amylase Activity and Specificity. *Biochemistry* **2008**, *47*, 3332–3344. [CrossRef]
41. Bohacek, R.S.; McMartin, C.; Guida, W.C. The art and practice of structure-based drug design: A molecular modeling perspective. *Med. Res. Rev.* **1996**, *16*, 3–50. [CrossRef]
42. Hopkins, A.L.; Keserü, G.M.; Leeson, P.D.; Rees, D.C.; Reynolds, C.H. The role of ligand efficiency metrics in drug discovery. *Nat. Rev. Drug Discov.* **2014**, *13*, 105–121. [CrossRef]
43. Ha, N.V.; Dat, D.T.; Nguyet, T.T. Stereoelectronic Properties of 1,2,4-Triazole-Derived N-heterocyclic Carbenes—A Theoretical Study. *VNU J. Sci. Nat. Sci. Technol.* **2019**, *35*, 55–62. [CrossRef]
44. Molecular Operating Environment (MOE) C.C.G.U., 1010 Handbook St. West, Suite 910, Montreal, QC, Canada, H3A 2R7. 2017. Available online: <https://www.chemcomp.com/index.htm> (accessed on 1 November 2021).
45. Saravanan, R.; Pari, L. Antihyperlipidemic and antiperoxidative effect of Diasulin, a polyherbal formulation in alloxan induced hyperglycemic rats. *BMC Complementary Altern. Med.* **2005**, *5*, 14. [CrossRef] [PubMed]
46. Adam, S.H.; Giribabu, N.; Rao, P.V.; Sayem, A.S.M.; Arya, A.; Panichayupakaranant, P.; Korla, P.K.; Salleh, N. Rhinacanthin C ameliorates hyperglycaemia, hyperlipidemia and pancreatic destruction in streptozotocin–nicotinamide induced adult male diabetic rats. *Eur. J. Pharmacol.* **2016**, *771*, 173–190. [CrossRef] [PubMed]
47. Rajasekaran, S.; Ravi, K.; Sivagnanam, K.; Subramanian, S. Beneficial effects of Aloe vera leaf gel extract on lipid profile status in rats with streptozotocin diabetes. *Clin. Exp. Pharmacol. Physiol.* **2006**, *33*, 232–237. [CrossRef] [PubMed]

48. Stewart, J.J. Optimization of parameters for semiempirical methods VI: More modifications to the NDDO approximations and re-optimization of parameters. *J. Mol. Modeling* **2013**, *19*, 1–32. [[CrossRef](#)]
49. Fernandes, N.P.; Lagishetty, C.V.; Panda, V.S.; Naik, S.R. An experimental evaluation of the antidiabetic and antilipidemic properties of a standardized *Momordica charantia* fruit extract. *BMC Complementary Altern. Med.* **2007**, *7*, 29. [[CrossRef](#)] [[PubMed](#)]
50. Bodade, S.S.; Shaikh, K.S.; Kamble, M.S.; Chaudhari, P.D. A study on ethosomes as mode for transdermal delivery of an antidiabetic drug. *Drug Deliv.* **2013**, *20*, 40–46. [[CrossRef](#)] [[PubMed](#)]
51. Alminderej, F.; Bakari, S.; Almundarij, T.I.; Snoussi, M.; Aouadi, K.; Kadri, A. Antioxidant Activities of a New Chemotype of *Piper cubeba* L. Fruit Essential Oil (Methyleugenol/Eugenol): In Silico Molecular Docking and ADMET Studies. *Plants* **2020**, *9*, 1534. [[CrossRef](#)]
52. Abrahamse, H.; George, S. Redox Potential of Antioxidants in Cancer Progression and Prevention. *Antioxidants* **2020**, *9*, 1156.
53. Famuyiwa, S.O.; Sanusi, K.; Faloye, K.O.; Yilmaz, Y.; Ceylan, Ü. Antidiabetic and antioxidant activities: Is there any link between them? *New J. Chem.* **2019**, *43*, 13326–13329. [[CrossRef](#)]
54. Gandhi, G.R.; Sasikumar, P. Antidiabetic effect of *Merremia emarginata* Burm. F. in streptozotocin induced diabetic rats. *Asian Pac. J. Trop. Biomed.* **2012**, *2*, 281–286. [[CrossRef](#)]
55. Pareek, H.; Sharma, S.; Khajja, B.S.; Jain, K.; Jain, G. Evaluation of hypoglycemic and anti-hyperglycemic potential of *Tridax procumbens* (Linn.). *BMC Complementary Altern. Med.* **2009**, *9*, 48. [[CrossRef](#)] [[PubMed](#)]
56. Gadadare, R.; Mandpe, L.; Pokharkar, V. Ultra rapidly dissolving repaglinide nanosized crystals prepared via bottom-up and top-down approach: Influence of food on pharmacokinetics behavior. *AAPS PharmSciTech* **2015**, *16*, 787–799. [[CrossRef](#)] [[PubMed](#)]
57. Sharma, M.; Kohli, S.; Dinda, A. In-vitro and in-vivo evaluation of repaglinide loaded floating microspheres prepared from different viscosity grades of HPMC polymer. *Saudi Pharm. J.* **2015**, *23*, 675–682. [[CrossRef](#)] [[PubMed](#)]